Journal of Sound and Vibration (2001) **242**(4), 629–640
doi:10.1006/jsvi.2000.3383, available online at http://www.idealibrary.com on IDEAL®

DYNAMIC RESPONSE OF A ROD DUE TO A MOVING HEAT SOURCE UNDER THE HYPERBOLIC HEAT CONDUCTION MODEL

N. S. AL-HUNITI

Mechanical Engineering Department, University of Jordan, Amman, Jordan

AND

M. A. AL-NIMR AND M. NAJI

Mechanical Engineering Department, Jordan University of Science and Technology, Irbid, Jordan

(*Received* 23 *March* 2000, *and in final form* 21 *August* 2000)

The dynamic thermal and elastic behavior of a rod due to a moving heat source are investigated. The hyperbolic heat conduction model is used for the prediction of the temperature history. Thermally induced displacements and stresses are determined. An analytical–numerical technique based on the Laplace transformation and the Riemann-sum approximation is used to calculate the temperature, displacement and stress distributions within the rod. The effects of different parameters such as the moving source speed, the convection heat transfer coefficient are studied and presented.

1. INTRODUCTION

Heat conduction problems involving a moving source have numerous engineering applications, such as welding, grinding, metal cutting, firing a bullet in a gun barrel, flame or laser hardening of metals, and others. In the literature, many researchers have investigated the heat transfer in solids with moving heat sources and under the effect of the classical Fourier heat conduction model [1–5].

More recently, lasers, because of their ability to produce high-power beams, have found applications in welding, drilling, cutting, machining of brittle materials, and surface hardening of metallic alloys. For example, in surface hardening, a high-power laser beam scans over the surface and unique metallurgical structures may be produced by rapid cooling that occurs subsequent to the laser heating.

In applications involving high heating rates induced by a short-pulse laser, the typical response time is in the order of picoseconds [6–9]. In such applications, the classical Fourier heat conduction model fails, and the use of the Cattaneo–Vernotte constitution is essential [10, 11]. In this constitution, it is assumed that there is a phase-lag between the heat flux vector ($\mathbf{q}$) and the temperature gradient (∇T). As a result, this constitution is given as

$$\mathbf{q} + \bar{\tau}\,\partial\mathbf{q}/\partial t = -k\nabla T, \tag{1}$$

where k is the thermal conductivity and $\bar{\tau}$ is the relaxation time (phase lag in heat flux). As a result, the energy equation under this constitution is written as

$$\rho c\bar{\tau}\,\partial^2 T/\partial t^2 + \rho c\,\partial T/\partial t = k\nabla^2 T. \tag{2}$$

0022-460X/01/190629 + 12 $35.00/0

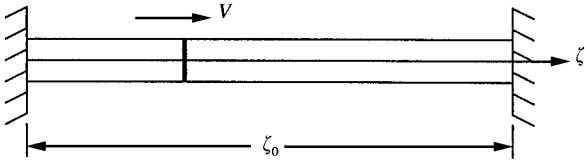

Figure 1. Schematic diagram of the rod under a moving heat source.

In the literature, numerous works have investigated the heat transfer in thin metallic domains under the effect of the hyperbolic heat conduction model [12–15].

Thermally induced deformation in structures occurs when a considerable temperature change takes place. Depending on the way structures are constrained, deformation may cause different types of distortions, or stress waves might develop. Transient deformation and stress waves are the major cause of thermal damage in laser processing of materials [16]. Therefore, this subject has been studied by many researchers. In most cases, however, the classical parabolic (diffusion) heat conduction model is used [17,18]. Dynamic variation of deflections and thermal stresses in a thin plate due to a very fast rate of heating under the hyperbolic heat conduction model was studied by Al-Huniti and Al-Nimr [19]. Kukla [20] has presented a solution to the problem of thermally induced vibration of a beam due to a moving heat source (laser beam), where he uses the parabolic heat conduction model.

To the authors' knowledge, the behavior of metallic domains involving moving laser-heating sources, under the effect of the hyperbolic heat conduction model, has not been investigated yet. The aim of the present work is to investigate the dynamic behavior of a metal rod heated by a high-power moving laser beam. The effect of the source speed, intensity, material properties and dimensions, and other parameters on the rod thermal behavior is investigated.

2. ANALYSIS

Consider the rod shown in Figure 1. The rod is of uniform cross-sectional area A_c and constant perimeter p. Initially, the rod is maintained at a uniform ambient temperature T_∞ and suddenly, a heating source starts to evolve its energy while moving in the axial direction. The thermal behavior of the rod is assumed to be lumped in the transverse direction and, as a result, the temperature T is a function of only time and the axial coordinate. The governing equations of the problem under consideration are

$$\rho c\,\partial T/\partial t = -\partial q/\partial x - (hp/A_c)(T-T_\infty) + g, \tag{3}$$

$$q + \bar{\tau}\,\partial q/\partial t = -k\,\partial T/\partial x. \tag{4}$$

Elimination of q between equations (3) and (4) yields

$$\bar{\tau}\rho c\frac{\partial^2 T}{\partial t^2} + \rho c\frac{\partial T}{\partial t} + \frac{\bar{\tau}hp}{A_c}\frac{\partial}{\partial t}(T-T_\infty) + \frac{hp}{A_c}(T-T_\infty) = g + \bar{\tau}\frac{\partial g}{\partial t} + k\frac{\partial^2 T}{\partial x^2}. \tag{5}$$

In the above equations, ρ is the mass density, c is the specific heat, h is the convection coefficient, $(hp/A_c)(T-T_\infty)$ represents the convection losses from the circumferential surface area of the rod and $g(t,x)$ represents a moving plane heat source of constant strength releasing its energy continuously while moving along the positive direction of the

x-axis with a constant velocity (v). This moving heat source is given as [3]

$$g(t, x) = g_0 \delta(x - vt), \tag{6}$$

where g is the heat source in W/m^3 and δ is the delta function. (A list of nomenclature is given in the Appendix.)

Equation (5) has the following initial and boundary conditions:

$$T(0, x) = T_0, \quad \frac{\partial T}{\partial t}(0, x) = 0, \quad \frac{\partial T}{\partial x}(t, 0) = \frac{\partial T}{\partial x}(t, x_0) = 0. \tag{7}$$

Here x_0 represents the length of the rod. The following dimensionless parameters are used in equation (5):

$$\theta = \frac{T - T_\infty}{T_\infty}, \quad \eta = \frac{t}{t_0}, \quad \tau = \frac{\bar{\tau}}{t_0}, \quad \zeta = \frac{x}{\sqrt{\kappa t_0}}, \quad V = \frac{v}{\sqrt{\kappa / t_0}}. \tag{8}$$

Here θ is the dimensionless temperature, T_∞ is the rod initial temperature (which is the same as the ambient temperature), η is the dimensionless time, t_0 is a reference time given by $t_0 = (D/2)^2/\kappa$, D is the diameter of the rod, κ is the thermal diffusivity, and τ is the dimensionless phase lag. In terms of the defined dimensionless parameters, equations (5) and (7) are rewritten as

$$\frac{\partial^2 \theta}{\partial \zeta^2} - \tau \frac{\partial^2 \theta}{\partial \eta^2} - (1 + \beta\tau) \frac{\partial \theta}{\partial \eta} - \beta\theta = -\gamma \delta\left(\eta - \frac{\zeta}{V}\right) - \tau\gamma \frac{\partial \delta}{\partial \eta}\left(\eta - \frac{\zeta}{V}\right), \tag{9}$$

$$\theta(0, \zeta) = 0, \frac{\partial \theta}{\partial \eta}(0, \zeta) = 0, \frac{\partial \theta}{\partial \zeta}(\eta, 0) = 0, \frac{\partial \theta}{\partial \zeta}(\eta, \zeta_0) = 0. \tag{10}$$

In equation (9), $\beta = (hpt_o)/A_c \rho c$ and $\gamma = (g_0 \sqrt{t_0})/VT_\infty \rho c \sqrt{\kappa}$.

Now, with the notation that Laplace transformation of $\theta(\eta, \zeta)$ is given by $\ell\{\theta(\eta, \zeta)\} = \bar{\theta}(s, \zeta)$, equations (9, 10) are transformed to

$$\frac{\mathrm{d}^2 \bar{\theta}(s, \zeta)}{\mathrm{d}\zeta^2} - [\tau s^2 + (1 + \beta\tau)s + \beta] \bar{\theta}(s, \zeta) = -\gamma(1 + \tau s) \mathrm{e}^{-(s/V)\zeta}, \tag{11}$$

$$\mathrm{d}\bar{\theta}(s, 0)/\mathrm{d}\zeta = \mathrm{d}\bar{\theta}(s, \zeta_0)/\mathrm{d}\zeta = 0. \tag{12}$$

Equations (11, 12) have the solution

$$\bar{\theta}(s, \zeta) = C_1 \mathrm{e}^{-\sqrt{A}\zeta} + C_2 \mathrm{e}^{\sqrt{A}\zeta} + C_3 \mathrm{e}^{-(s/V)\zeta}, \tag{13}$$

where

$$A = \tau s^2 + (1 + \beta\tau)s + \beta, \quad C_3 = \frac{\gamma(1 + \tau s)}{A - s^2/V^2}, \tag{14, 15}$$

$$C_1 = \frac{s}{V\sqrt{A}} \left(\frac{\mathrm{e}^{-(s/V)\zeta_0} - \mathrm{e}^{\sqrt{A}\zeta_0}}{\mathrm{e}^{\sqrt{A}\zeta_0} - \mathrm{e}^{-\sqrt{A}\zeta_0}} \right) C_3, \quad C_2 = C_1 + \left(\frac{s}{V\sqrt{A}} \right) C_3. \tag{16, 17}$$

The rod used in the analysis is very thin. This implies that there is no neighboring medium in the lateral directions (y and z) and hence, the Poisson effect is negligible. This reduces the problem to the one-dimensional case of stress and strain. Based on this, the stress–strain relation for the rod under consideration (including the effect of a temperature gradient) becomes

$$\sigma_x = E\varepsilon_x - E\alpha(T - T_\infty), \tag{18}$$

where E is the modulus of elasticity and α is the coefficient of thermal expansion. The one-dimensional strain–displacement relation is

$$\varepsilon_x = \partial u/\partial x, \tag{19}$$

where u is the rod elastic displacement in the longitudinal (x) direction. The one-dimensional equation of motion for an elastic solid is given by

$$\partial\sigma_x/\partial x = \rho\,\partial^2 u/\partial t^2. \tag{20}$$

Substituting equations (18, 19) into equation (20) results in the governing equation (wave equation):

$$\frac{\partial^2 u(t,x)}{\partial x^2} - \frac{\rho}{E}\frac{\partial^2 u(t,x)}{\partial t^2} = \alpha\frac{\partial T(t,x)}{\partial x}. \tag{21}$$

A dimensionless displacement of the rod is defined as

$$U = \frac{\sqrt{E/\rho}}{\alpha\kappa T_\infty}\,u. \tag{22}$$

Upon using this and the parameters defined in equations (8), the dimensionless form of equation (21) becomes

$$\frac{\partial^2 U(\eta,\zeta)}{\partial\zeta^2} - \lambda_1\frac{\partial^2 U(\eta,\zeta)}{\partial\eta^2} = \lambda_2\frac{\partial\theta(\eta,\zeta)}{\partial\zeta}, \tag{23}$$

where $\lambda_1 = \rho\kappa/Et_0$ and $\lambda_2 = 1/\sqrt{\lambda_1}$.

Upon assuming that the rod was initially at rest in the undeformed position, equation (23) is subject to the initial conditions

$$U(0,\zeta) = 0, \quad \frac{\partial U}{\partial\eta}(0,\zeta) = 0. \tag{24}$$

With the rod assumed to be supported at both ends, the boundary conditions are given by

$$U(\eta,0) = 0, \quad U(\eta,\zeta_0) = 0. \tag{25}$$

With use of equations (24), the Laplace transform of equation (23) yields

$$\frac{\mathrm{d}^2\bar{U}(\zeta,s)}{\mathrm{d}\zeta^2} - \lambda_1 s^2\bar{U}(\zeta,s) = \lambda_2\frac{\mathrm{d}\bar{\theta}(\zeta,s)}{\mathrm{d}\zeta}, \tag{26}$$

where $\bar{U}(s,\zeta)$ is the Laplace transform of $U(\eta,\zeta)$. Differentiating equation (13) and substituting the reset into equation (26) results in

$$\frac{d^2\bar{U}(\zeta,s)}{d\zeta^2} - \lambda_1 s^2 \bar{U}(\zeta,s) = \lambda_2\left(-\sqrt{A}C_1 e^{-\sqrt{A}\zeta} + \sqrt{A}C_2 e^{\sqrt{A}\zeta} - (s/V)C_3 e^{-(s/V)\zeta}\right). \quad (27)$$

Also, the Laplace transform of equations (25) yields

$$\bar{U}(s,0) = 0, \quad \bar{U}(s,\zeta_0) = 0. \quad (28)$$

Equations (27, 28) have the solution

$$\bar{U}(\zeta,s) = C_4 e^{-\sqrt{\lambda_1 s}\zeta} + C_5 e^{\sqrt{\lambda_1 s}\zeta} + C_6 e^{-\sqrt{A}\zeta} + C_7 e^{\sqrt{A}\zeta} + C_8 e^{-(s/V)\zeta}, \quad (29)$$

where

$$C_6 = \frac{\lambda_2\sqrt{A}}{\lambda_1 s^2 - A} C_1, \quad C_7 = -\frac{\lambda_2\sqrt{A}}{\lambda_1 s^2 - A} C_2, \quad (30, 31)$$

$$C_8 = \frac{\lambda_2 s/V}{\lambda_1 s^2 - s^2/V^2} C_3, \quad (32)$$

$$C_4 = \frac{C_6(e^{\sqrt{\lambda_1 s}\zeta_0} - e^{-\sqrt{A}\zeta_0}) + C_7(e^{\sqrt{\lambda_1 s}\zeta_0} - e^{\sqrt{A}\zeta_0}) + C_8(e^{\sqrt{\lambda_1 s}\zeta_0} - e^{-(s/V)\zeta_0})}{e^{-\sqrt{\lambda_1 s}\zeta_0} - e^{\sqrt{\lambda_1 s}\zeta_0}}, \quad (33)$$

$$C_5 = -(C_4 + C_6 + C_7 + C_8). \quad (34)$$

Now, the dimensionless stress–displacement relation is rewritten in terms of equations (18) and (19) as

$$S_x(\eta,\zeta) = \lambda_3 \frac{\partial U(\eta,\zeta)}{\partial\zeta} - \theta(\eta,\zeta), \quad (35)$$

where $\lambda_3 = \sqrt{\lambda_1}$ and S_x is the dimensionless stress defined as

$$S_x = \sigma_x/E\alpha T_\infty. \quad (36)$$

The Laplace transform of equation (35) yields

$$\bar{S}_x(s,\zeta) = \lambda_3 \frac{d\bar{U}(s,\zeta)}{d\zeta} - \bar{\theta}(s,\zeta). \quad (37)$$

Substituting equations (13) and (29) into equation (37) yields the dimensionless stress as

$$\bar{S}_x(s,\zeta) = \lambda_3\{ -\sqrt{\lambda_1 s}C_4 e^{-\sqrt{\lambda_1 s}\zeta} + \sqrt{\lambda_1 s}C_5 e^{\sqrt{\lambda_1 s}\zeta} - \sqrt{A}C_6 e^{-\sqrt{A}\zeta} + \sqrt{A}C_7 e^{\sqrt{A}\zeta} - (s/V)C_8 e^{-(s/V)\zeta}\} - \{C_1 e^{-\sqrt{A}\zeta} + C_2 e^{\sqrt{A}\zeta} + C_3 e^{-(s/V)\zeta}\}. \quad (38)$$

3. SOLUTION

In order to determine the temperature, displacement and stress histories of the rod equations (13), (29) and (38) must be inverted back into the time domain. However, these

TABLE 1

Properties of copper

$\bar{\tau}$	4·348 (10^{-13}) s
κ	1·1283 (10^{-4}) m^2/s
c	385 J/(K kg)
α	1·76 (10^{-5}) 1/K
E	1·19 (10^{11}) N/m^2
ρ	8960 kg/m^3

equations are too complicated to be inverted directly and hence, no closed-form solutions are possible. Therefore, the Riemann-sum approximation method is used. In this method, any function $\bar{\theta}(s, \zeta)$ is inverted to the time domain as [16]

$$\theta(\eta, \zeta) = \frac{e^{\varepsilon\eta}}{\eta}\left(\frac{1}{2}\bar{\theta}(\varepsilon, \zeta) + \mathrm{Re}\sum_{n=1}^{N}\bar{\theta}\left(\varepsilon + \frac{in\pi}{\eta}, \zeta\right)(-1)^n\right), \tag{39}$$

where Re is the real part and i is the complex number $\sqrt{-1}$. For faster convergence, numerous numerical experiments have shown that the value of ε satisfying the relation ($\varepsilon\eta \approx 4{\cdot}7$) gives the most satisfactory results [16].

4. RESULTS AND DISCUSSION

Numerical calculations are performed on a copper rod for which the properties are given in Table 1. The temperature variations in both time and space are first determined, then the displacement, and finally the stress variations.

Figure 2 shows the transient thermal behavior of the mid-point of the rod ($\zeta = 25$) at different moving heat source speeds. For the same time duration, the source evolves the same amount of energy. However, the intensity of this released energy per unit rod length decreases as the source speed increases. As a result, each specified location receives less amount of energy as the source speed increases. This in turn leads to a reduction in the local temperature distribution within the rod. From the qualitative behavior of the source $\gamma\delta(\eta - \zeta/V)$, the source releases its energy at time $\eta = \zeta/V$. This time varies as ζ varies, but as V increases, the source releases its energy during the early stages of time. This shifts the peak in the rod temperature toward small values of η as V increases. Also, the rod thermal behavior is insensitive to the variation of heating source speed at large speeds and times. At very large moving source speeds, the source traces the whole length of the rod within almost the same time, which is a very small one. Also, at very large speeds, the rod thermal behavior attains an asymptotic behavior as clear from the same figure.

Figure 3 shows the spatial variation in rod temperature at different moving source speeds. This figure is another point of view for the results of Figure 2. It is worth mentioning here that the temperature peaks for large speed are shifted toward the very near end of the rod (at $\zeta \to 0$) and this is the reason why these peaks do not appear clearly. For large speeds of the moving heat source, the source evolves its energy almost instantaneously within all locations of the rod. As a result, the spatial variations in the rod temperature disappear and the rod may be treated as a lumped system from a thermal point of view. Mathematically, for large speed, V, the source term, $\delta(\eta - \zeta/V)$, becomes $\delta(\eta)$. This implies that the source term becomes independent of space.

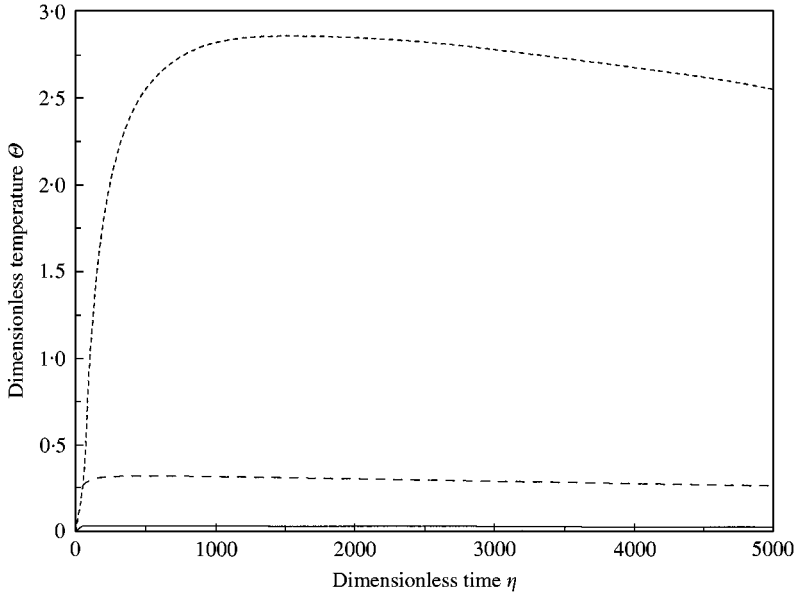

Figure 2. Transient variations of dimensionless temperature with time at different source speeds for $\zeta = 25$ and $\beta = 5{\cdot}1385 * 10^{-5}$. -----, $V = 0{\cdot}8863$; ———, $V = 8{\cdot}863$; ———, $V = 88{\cdot}63$.

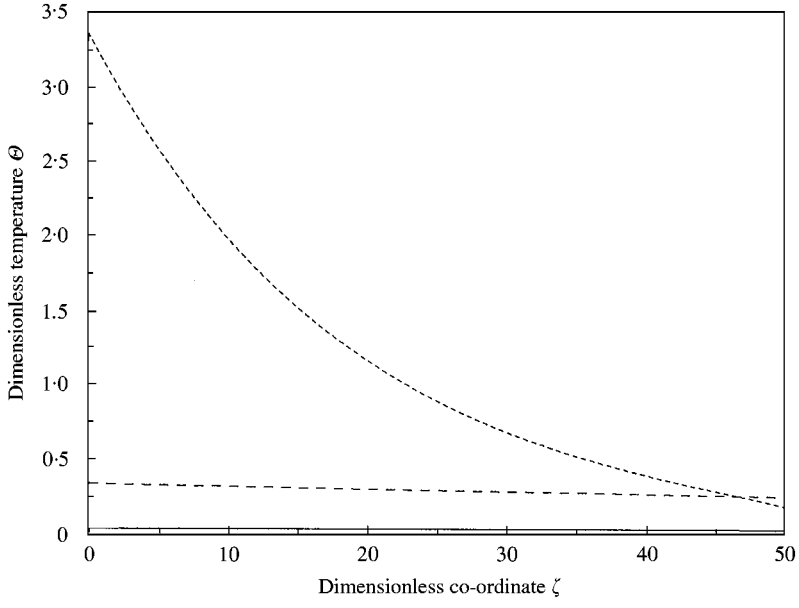

Figure 3. Transient variations of dimensionless temperature along the rod length at different source speeds for $\eta = 100$ and $\beta = 5{\cdot}1385 * 10^{-5}$. -----, $V = 0{\cdot}8863$; ———, $V = 8{\cdot}863$; ———, $V = 88{\cdot}63$.

Figure 4 shows the effect of the dimensionless heat convective losses on the rod thermal behavior. As β increases, the thermal losses from the rod increase and the rod temperature decreases. This reduction enhances as time proceeds due to the accumulation in the effect of β. Also, it is clear that the convective losses have insignificant effect on the rod thermal behavior during very early stages of time.

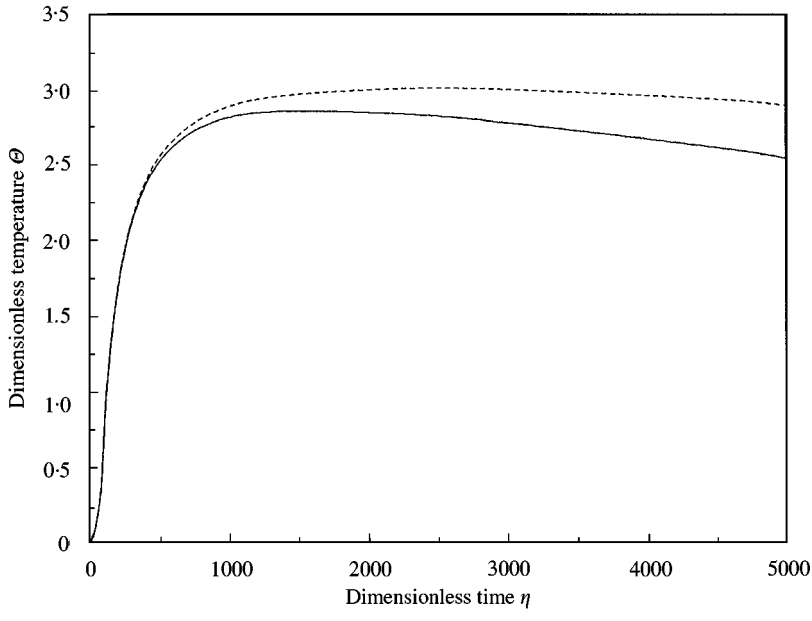

Figure 4. Transient variations of dimensionless temperature with time at different values of convective heat transfer coefficient for $\zeta = 25$ and $V = 0{\cdot}8863$. ——, $\beta = 5{\cdot}1385{*}10^{-5}$; -----, $\beta = 2{\cdot}5693{*}10^{-5}$.

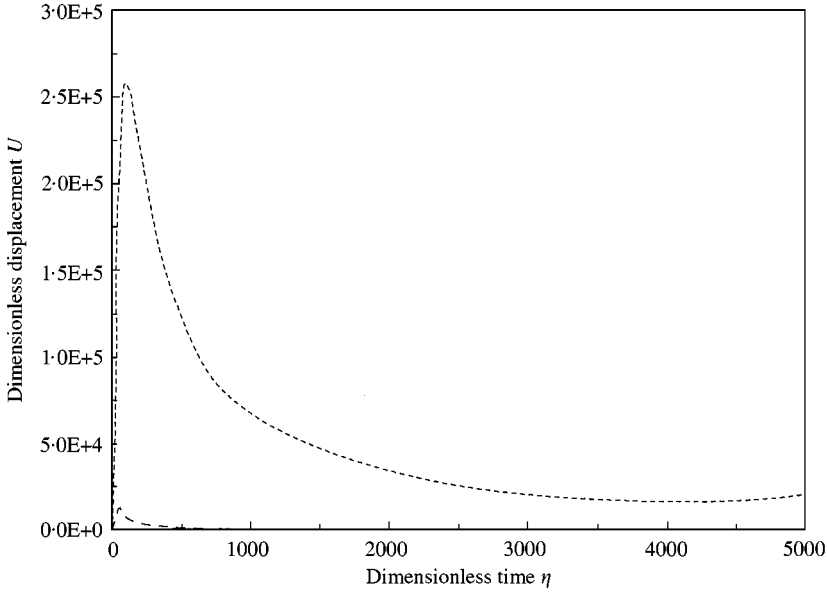

Figure 5. Transient variations of dimensionless displacement with time at different source speeds for $\zeta = 25$ and $\beta = 5{\cdot}1385{*}10^{-5}$. -----, $V = 0{\cdot}8863$; ———, $V = 8{\cdot}863$; ——, $V = 88{\cdot}63$.

Figure 5 shows the time history of the thermally induced displacement of the midpoint of the rod at different moving heat source speeds. It can be seen from this figure that the amount of the displacement increases as the source speed decreases. This is mainly due to higher temperature at lower speeds (see Figure 2). Also, it can be noticed that at very large

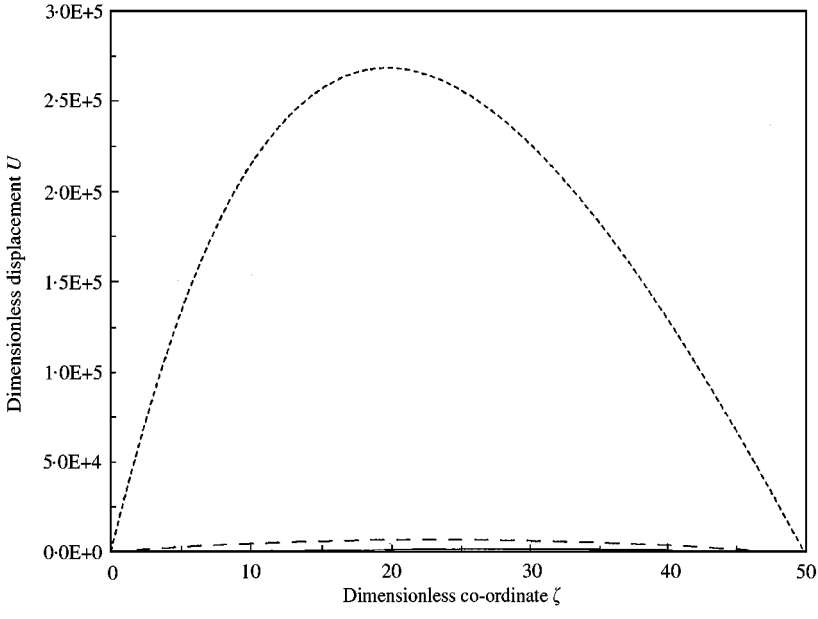

Figure 6. Transient variations of dimensionless displacement along the rod length at different source speeds for $\eta = 100$ and $\beta = 5{\cdot}1385 * 10^{-5}$. -----, $V = 0{\cdot}8863$; ———, $V = 8{\cdot}863$; ———, $V = 88{\cdot}63$.

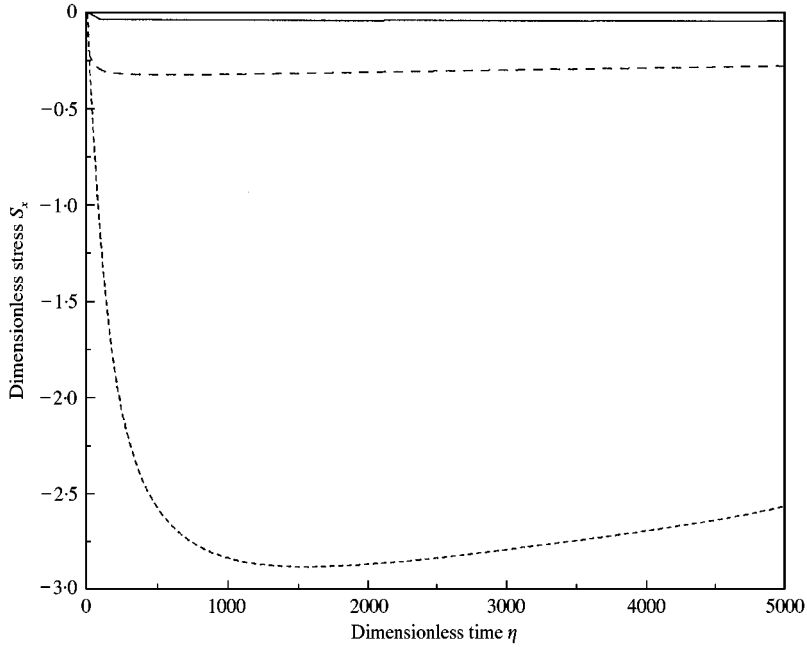

Figure 7. Transient variations of dimensionless stress with time at different source speeds for $\zeta = 25$ and $\beta = 5{\cdot}1385 * 10^{-5}$. -----, $V = 0{\cdot}8863$; ———, $V = 8{\cdot}863$; ———, $V = 88{\cdot}63$.

speeds, there is almost no induced displacement in the rod. Figure 6 shows the spatial variation of the displacement. Again, this figure is another point of view of Figure 5.

Figures 7 and 8 show the stress variation with time and space, respectively. Since this rod is restrained against motion from both ends, the thermally induced stresses develop and

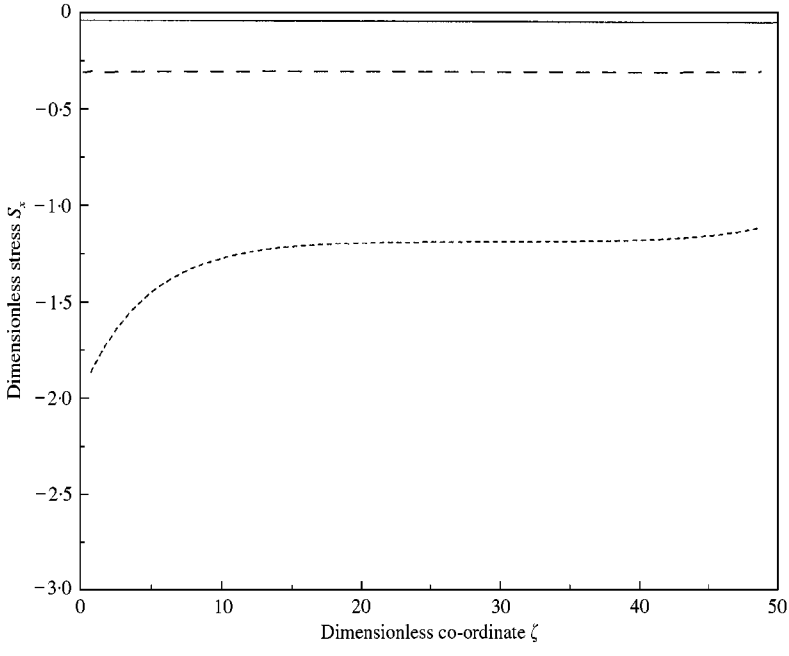

Figure 8. Transient variations of dimensionless stress along the rod length at different source speeds for $\eta = 100$ and $\beta = 5{\cdot}1385 * 10^{-5}$. -----, $V = 0{\cdot}8863$; ———, $V = 8{\cdot}863$; ———, $V = 88{\cdot}63$.

their magnitudes depend on the temperature difference. This is clear from these two figures as the stress behavior follows that of the temperature. It is worth mentioning that because of the end restraints, the developed thermal stresses are compressive since these restraints oppose the rod elongation. It can be seen here that, as was concluded in the thermal behavior, for large values of speed, the variations in the rod stress disappear and the system may be treated as a lumped system.

5. CONCLUDING REMARKS

The dynamic thermal and elastic behavior of a rod involving a moving heat source is modelled. The hyperbolic heat conduction model is used to determine the thermal behavior of the thin rod.

The governing equations are derived and solved by using the Laplace transformation technique. The solutions in the Laplace domain are inverted numerically by using the Riemann-sum approximation.

The effects of different geometrical, operating and design parameters on the thermal and elastic behavior of the rod are investigated. The temperature of the rod is found to decrease at large source speeds while the effect of this speed on the thermal behavior is insignificant at very large time. Also, it is found that convective losses have insignificant effect on the rod during very early stages of time. However, these losses accumulate with time and affect the thermal behavior.

The behavior of the thermally induced displacement and stress of the rod is found to depend on the source speed in the same manner as that of the temperature behavior for the source speeds considered. At large values of speed, the variations in the rod thermal and elastic behavior disappear and the rod may be treated as a lumped system.

REFERENCES

1. C. K. HSIEH 1995 *American Society of Mechanical Engineers Journal of Heat Transfer* **117**, 1076–1078. Exact solution of Stefan problems related to a moving line heat source in a quasi-stationary state.
2. C. K. HSIEH 1995 *International Journal of Heat and Mass Transfer* **38**, 71–79. Exact solution of Stefan problems for a heat front moving at constant velocity in a quasi-steady state.
3. M. N. OZISIK 1993 *Heat conduction* New York: Wiley, 2nd edition.
4. A. NEHAD 1995 *International Communications in Heat and Mass Transfer* **22**, 779–790. Enthalpy technique for solution of Stefan problems: Application to the keyhole plasma arc welding process involving moving heat source.
5. D. ROSENTHAL 1946 *Transaction of the American Society of Mechanical Engineers* **68**, 849–866. The theory of moving sources of heat and its application to metal treatments.
6. T. Q. QIU and C. L. TIEN 1992 *International Journal of Heat and Mass Transfer* **35**, 719–726. Short-pulse laser heating on metals.
7. T. Q. QIU and C. L. TIEN 1993 *American Society of Mechanical Engineers Journal of Heat Transfer* **115,** 835–841. Heat transfer mechanism during short pulse laser heating of metals.
8. M. A. AL-NIMR and V. S. ARPACI 1999 *Journal of Applied Physics* **85**, 2517–2521. Picosecond thermal pulses in thin metal films.
9. M. A. AL-NIMR 1997 *International Journal of Thermophysics* **18**, 1257–1268. Heat transfer mechanisms during short-duration laser heating of thin metal films.
10. C. CATTENEO 1958 *Compte Rendus* **247**, 431–433. A form of heat conduction equation which eliminates the paradox of instantaneous propagation.
11. P. VERNOTTE 1961 *Compte Rendus* **252**, 2190–2191. Some possible complications in the phenomenon of thermal conduction.
12. M. A. AL-NIMR and M. NAJI 1999 *Heat and Mass Transfer* **35**, 493–497. The hyperbolic heat conduction equation in an anisotropic material.
13. H. T. CHEN and J. Y. LIN 1994 *International Journal of Heat and Mass Transfer* **37**, 153–164. Analysis of two-dimensional hyperbolic heat conduction problems.
14. W. S. KIM, L. G. HECTOR and M. N. OZISIK 1990 *Journal of Applied Physics* **68**, 5478–5485. Hyperbolic heat conduction due to axisymmetric continuous or pulsed heat sources.
15. B. VICK and M. OZISIK 1983 *American Society of Mechanical Engineers Journal of Heat Transfer* **105**, 902–907. Growth and decay of a thermal pulse predicted by the hyperbolic heat conduction equation.
16. D. TZOU 1997 *Macro-to-Microscale Heat Transfer*. Washington, DC: Taylor and Francis.
17. B. BOLEY and J. WEINER 1985 *Theory of Thermal Stresses*. FL: Krieger.
18. W. NOWACKI 1986 *Thermoelasticity*. Warsaw: Pergamon Press, PWN.
19. NASER S. AL-HUNITI and M. A. AL-NIMR 2000 *Journal of Thermal Stresses* **23**, 293–307. Behavior of thermal stresses in a rapidly-heated thin plate.
20. J. KIDAWA-KUKLA 1997 *Journal of Sound and Vibration* **205**, 213–222. Vibration of a beam induced by harmonic motion of a heat source.

APPENDIX A: NOMENCLATURE

A_c	cross-sectional area, m^2
c	specific heat, J/(K kg)
g	heating source term, W/m^3
g_0	strength of the heating source term, W/m^2
h	convective heat transfer coefficient, $W/(m^2\,K)$
i	complex number $= \sqrt{-1}$
k	thermal conductivity, W/(m K)
p	perimeter, m
q	heat flux vector, W/m^2
s	Laplacian parameter
S_x	dimensionless stress, $(\sigma_x/E\alpha T_\infty)$
t	time, s
t_0	reference time

T	temperature, K
T_∞	ambient and initial temperature, K
v	speed of the moving source, m/s
V	dimensionless speed of the moving source, $(v/\sqrt{\kappa/t_0})$
x	axial coordinate, m
x_0	length of the rod, m

Greek letters

δ	delta function, l/m
η	dimensionless time, t/t_0
γ	dimensionless parameter, $(g_0\sqrt{t_0}/VT_\infty\rho c\sqrt{\kappa})$
θ	dimensionless temperature, $(T-T_\infty)/T_\infty$
$\overline{\theta}$	Laplace transformation of dimensionless temperature
κ	thermal diffusivity, m^2/s
ρ	mass density, kg/m^3
σ_x	longitudinal stress, N/m^2
$\bar{\tau}$	phase lag, s
τ	dimensionless phase lag, $\bar{\tau}/t_0$
ζ	dimensionless axial coordinate, $x/\sqrt{\kappa t_0}$
ζ_0	dimensionless length of the rod, $x_0/\sqrt{\kappa t_0}$